Evolution of fungal phenotypic disparity

By THOMAS J. SMITH[1*] & PHILIP C. J. DONOGHUE[1]

[1]Bristol Palaeobiology Group, School of Earth Sciences, University of Bristol, Life Sciences Building, Tyndall Avenue, Bristol, BS8 1TQ, UK

*Corresponding author

Correspondence: tom.smith@bristol.ac.uk

Abstract

Organismal grade multicellularity has been achieved only in animals, plants, and fungi. All three kingdoms manifest phenotypically disparate body plans, but their evolution has only been considered in detail for animals. Here we test the general relevance of hypotheses on the evolutionary assembly of animal body plans by characterising the evolution of fungal phenotypic variety (disparity). The distribution of living fungal form is defined by four distinct morphotypes: flagellated, zygomycetous, sac-bearing, and club-bearing. The discontinuity between morphotypes is a consequence of extinction, indicating that a complete record of fungal disparity would present a more homogeneous distribution of form. Fungal disparity expands episodically through time, punctuated by a sharp increase associated with the emergence of multicellular body plans. Simulations show these temporal trends to be non-random and at least partially shaped by hierarchical contingency. These trends are decoupled from changes in gene number, genome size, and taxonomic diversity. Only differences in organismal complexity, characterised as the number of traits that constitute an organism, exhibit a meaningful relationship with fungal disparity. Both animals and fungi exhibit episodic increases in disparity through time, resulting in distributions of form made discontinuous by extinction. These congruences suggest a common mode of multicellular body plan evolution.

Keywords:

Fungi, disparity, phenotype, evolution, morphology, complexity, multicellularity

Introduction

The evolution of multicellular organisms from unicellular ancestors is widely recognised as a major evolutionary transition[1, 2]. However, the 25 lineages[3] in which we know multicellularity to have emerged do not appear to be imbued with the same evolutionary potential. Just three lineages, animals, plants, and fungi, have achieved organismal grade multicellularity and, in doing so, manifested an unparalleled diversity of body plans, the evolutionary origins of which have long been the subject of controversy. Analyses of animals have revealed that the range of multicellular body plans is discontinuous, with clusters of self-similar organisms separated by unoccupied regions of design space variably rationalised as being representative of unexplored, extinct, or theoretically impossible phenotypes[4-6]. Furthermore, many analyses of animal phenotypic diversity (i.e. disparity) have revealed that clades tend to achieve their greatest disparity early in their evolutionary history[4, 5, 7, 8]. However, whether these are general patterns that should be anticipated of all organismal grade multicellular lineages is unclear because of a paucity of studies in other clades. Fungi are the second-most taxonomically diverse multicellular kingdom, represented by an estimated 5.1 million species[9]. Phylogenomics has revolutionised perceptions of fungal phylogeny[10-13], revealing a kingdom comprised of nine major lineages: the zoosporic Opisthosporidia (Fig. 1A-B), Blastocladiomycota (Fig. 1C), Chytridiomycota (Fig. 1D), and Neocallimastigomycota (Fig. 1E); the zygomycetous Glomeromycota (Fig. 1F), Mucoromycota (Fig. 1G), and Zoopagomycota (Fig. 1H-I); and the dikaryotic Basidiomycota (Fig. 1K-J) and Ascomycota (Fig. 1L-M). However, the pattern of phenotypic diversification that accompanies the emergence and radiation of these lineages is uncharacterised.

With the aim of obtaining generalisable insights into the patterns and processes underlying the origin and diversification of organismal-grade multicellular body plans, we characterise the evolution of phenotypic disparity in fungi. We map these phylogenetic interrelationships across fungal morphospace to understand the mode by which the overall distribution of disparity is achieved. As subcellular characters are regularly used to differentiate fungal taxa in studies of diversity, we explore how much they contribute to the overall occupation of fungal morphospace in comparison to cellular and multicellular features. We also investigate how these distributions of form relate to other measures of evolution, specifically organismal complexity and taxonomic diversity. We characterize disparity-through-time to assess whether fungi achieve their maximum disparity early in their evolutionary history. We use simulations to test whether these patterns deviate from null expectations of our phylogenetic sample. Finally, we seek to explain the cause of the patterns recovered by testing whether increases in disparity accompany genomic expansion.

Results

Dikarya are the most morphologically disparate fungi

Fungal phenotypic variation was characterised using 303 discrete characters scored for 44 higher taxa, including two filose amoeboid outgroups. These data were sourced from the Assembling the Fungal Tree Of Life (AFTOL) database[14], a synthesis of our understanding of subcellular phenotypic variation in fungi, together with the wider literature. All higher taxa included in a recent review of fungal diversity[13] with representation in the AFTOL database were sampled. This approach provided the best compromise between phenotypic data availability and representative sampling of fungal diversity. 110 of the characters sampled were autapomorphic

(i.e. were scored as absent or missing in all but one taxon). The overall impact of autapomorphies in analyses of disparity depends on how they are distributed among taxa but they nevertheless serve to differentiate morphologically unique organisms in morphospace, changing its structure in the process[15]. They allow for the characterisation of the full phenotypic range of a clade, so long as appropriate indices of disparity are employed[16], which is essential if meaningful insights into phenotypic evolution are to be derived. Alongside the autapomorphies, 15 characters in the dataset are invariant, reflecting primitive features shared by otherwise disparate body plans. As such, 288 characters contributed to the relative intertaxon distances derived from our analyses.

These data were ordinated using two different methods. The first, principal coordinate analysis (PCoA), ordinates data in such a way that the distribution of taxa along each resulting axis captures their relative similarity to one another. As such, when two or more of these axes are plotted to create a morphospace, taxa that cluster together are more phenotypically similar than those that plot further away. This metric quality of PCoA morphospace facilitates the quantitative characterisation of the distribution of taxa within it. A limitation of PCoA is that it can require large numbers of axes to capture the full variation of a multivariate dataset, which can make visualisation difficult. As such, we also use non-metric multidimensional scaling (NMDS) to ordinate our data along just two axes. While this facilitates a more intuitive visualisation of the data, the resulting morphospace is not metric, hence the resulting intertaxon distances lose their reliability as proxies for the phenotypic distinctiveness of taxa. However, the relative positions of taxa (e.g. whether they occupy overlapping or non-overlapping regions) in NMDS morphospace remain meaningful. We used both NMDS and PCoA to ordinate our data so that we could leverage the strengths of each method. 5 indices were used to characterise the distribution of fungi in PCoA morphospace: sum of ranges, which measures the divergence of peripheral

phenotypes; sum of variances and average Euclidean distance from centroid, which characterise the overall size of the explored area; average nearest neighbour Euclidean distance and average minimum spanning tree Euclidean distance, which characterise the density with which points cluster in an area of morphospace. In analyses where covariation between indices characterising the same aspect of morphospace was recovered, we characterize patterns in size and density using sum of ranges and average minimum spanning tree Euclidean distance respectively. The results as presented by the omitted indices can be found in the Extended Data.

Of the nine major fungal lineages, Ascomycota and Basidiomycota are united within Dikarya, the most diverse fungal clade[9]. Mucoromycota, Glomeromycota, and sometimes Zoopagomycota comprise the sister group of Dikarya; whether the latter phylum forms a clade or grade with the other taxa is uncertain[10, 13]. Chytridiomyceta, the monophyletic grouping of Chytridiomycota and Neocallimastigomycota, Blastocladiomycota, and Opisthosporidia represent successive sister taxa to the clade uniting all other fungi in most analyses[10, 17]. These lineages are distributed across morphospace in four non-overlapping clusters, each characterising distinct morphotypes (Fig. 2A): flagellated (Chytridiomycota, Blastocladiomycota, Neocallimastigomycota, Opisthosporidia, *Caulochytrium*, and Olpidiaceae), zygomycetous (Zoopagomycota, Glomeromycota, and Mucoromycota), club (Basidiomycota and Entorrhizomycotina) and sac (Ascomycota). These morphotypes are characterised by the presence of specific characters: the presence of a flagellum (flagellated), zygospore (zygomycetous), ascus (sac) and basidium (club). The NMDS visualisation is not congruent with the PCoA characterisation of fungal morphospace in terms of intertaxon distance. Club fungi occupy the largest area of PCoA morphospace (Fig. 2B). While the large interquartile range of sac fungi almost completely overlaps with that of club fungi, the median size of the area they occupy is much closer to those occupied by the non-

dikaryotic morphotypes. Accordingly, club fungi populate morphospace less densely than their sac-bearing counterparts. In contrast, the non-dikaryotic flagellated and zygomycetous fungi occupy smaller and more compact regions of morphospace. These differences are borne out when dikarya and non-dikaryotic fungi are compared directly; the former exhibit greater dispersal across morphospace than the latter. This quantification and visualisation of fungal morphospace serves as a modern census of fungal phenotypic diversity. However, a phylogenetic perspective is required to approach the evolutionary history of fungal disparity.

Divergence defines fungal morphospace occupation

To understand how this pattern in extant fungal phenotypic disparity was achieved over geologic time, we used stochastic character mapping on a re-coded version of the base dataset to estimate the phenotypes of hypothetical ancestors not observed in the living or fossil records. These estimated ancestors were then used to map the phylogenetic interrelationships of fungi across the NMDS visualisation of fungal morphospace, creating a phylomorphospace (Fig. 2A). Fossils were not included as their paucity makes proportionate sampling across the major fungal lineages impossible[18, 19]. The estimated ancestors bridge the gaps in morphospace between the four main clusters, indicating that the apparent isolation of sac, club, zygomycetous, and flagellated fungi is a product of the extinction of these phylogenetic intermediates. They also reveal the unidirectional radiation of fungi across morphospace; convergence only occurs within and not between the four morphotypes.

Subcellular phenotypes shape fungal morphospace

To test to what degree phylogenetically informative, subcellular phenotypes shape the overall distribution of fungi in morphospace, we partitioned our dataset into two subsets: one limited to

subcellular characters, the other sampling cellular and multicellular features only (hereafter, the supracellular subset). PCoA and NMDS were used to ordinate each of these subsets, and phylomorphospaces were constructed using the results of the latter. The subcellular subset characterises a fungal morphospace similar in structure to that of the complete dataset as each of the four morphotypes occupy distinct, non-overlapping regions (Fig. 2C). In terms of their relative size and density, the NMDS visualisation does not reflect the PCoA quantification of intertaxon distances well. Zygomycetous fungi occupy the largest area of PCoA morphospace, with the club, flagellated, and sac morphotypes populating successively smaller regions (Fig. 2D). Non-dikaryotic fungi occupy a larger area of subcellular PCoA morphospace than Dikarya. However, the differences between the four morphotypes are relatively small. This relative homogeneity extends to the density indices; the average nearest neighbour Euclidean distance and average minimum spanning tree Euclidean distance interquartile ranges for all four morphotypes show considerable overlap. Only the flagellated fungi present a consistent trend, as they generally exhibit the most compact distribution regardless of how it is characterised. In contrast, the relative densities of the other three morphotypes, and consequently that of Dikarya and non-dikaryotic fungi, are index-dependent. These differences likely stem from how the indices interact with the peripheral phenotype of Laboulbeniomycetes, as such taxa can have index-specific effects on perceptions of morphological disparity[16].

Ordination of the supracellular characters presents a different pattern to the complete dataset. While the four morphotypes occupy distinct areas of morphospace, the distance between the regions populated by flagellated and zygomycetous fungi is much smaller relative to that separating the two clusters from Dikarya (Fig. 2E). The NMDS visualisation is reasonably representative of the PCoA quantification of supracellular intertaxon distance, with the sac and

club fungi populating comparably expansive regions of morphospace, and the flagellated and zygomycetous occupying successively smaller, more compact areas (Fig. 2E-F). Accordingly, Dikarya occupy an area of supracellular morphospace considerably larger in size than that of non-dikaryotic fungi at a lower density. The contributions of estimated ancestral phenotypes and fungal phylogeny to perceptions of evolving morphological disparity did not deviate from the patterns presented by analyses of the complete dataset regardless of how the characters were subsetted.

Supracellular complexity may explain dikaryotic disparity

The concept of disparity, the variation in form presented by a group of organisms, is sometimes conflated with organismal complexity, the number of part types or the degree to which parts differ in an individual[20, 21]. However, these concepts are distinct; complexity is an intrinsic property of individuals, whereas disparity characterises variation between members of a group. As a greater number of parts facilitates greater differences between organisms, a link between the two concepts is rational[6]. Here we explore this relationship and test the assumption that increases in organismal complexity facilitate the exploration of new areas of morphospace through the evolution of novel phenotypes[22]. Three sets of complexity data were derived, one for each dataset (complete, subcellular, and supracellular). The characters in our dataset are one of two types: binary presence-absence, and multi-state characters codifying how many replicates of a specific phenotypic trait are present. As such, we operationalised complexity as the sum of the character scores for each taxon; an operationalisation compatible with existing definitions of horizontal complexity[20].

Mapping fungal complexity across the complete phylomorphospace indicates sac fungi are the most complex of the four morphotypes, while flagellated and zygomycetous forms are the least (Fig. 3A). The emergence of dikaryotic fungi corresponds to a general increase in fungal complexity. However, this pattern not evident in the evolution of zygomycetous fungi from their flagellated ancestors. These inconsistencies are reflected in the strength of the correlation between pairwise differences in organismal complexity and morphological distances (Fig. 3B).

Subcellular characters exhibit a weaker relationship between fungal complexity and morphospace occupation (Fig. 3C-D). Flagellated fungi exhibit comparable complexity to their dikaryotic counterparts, while zygomycetous lineages still appear marginally less complex. The significant but weak correlation recovered between the pairwise differences in complexity and morphological distances reflects this result (Fig. 3D). In contrast, supracellular characters exhibit a strong relationship between complexity and disparity (Fig. 3E-F). Supracellular complexity increases with the emergence of each morphotype, with flagellated fungi being the simplest and sac fungi the most complex. As such, it coincides with the episodic expansion of supracellular morphospace. Accordingly, pairwise differences in complexity correlate strongly with morphological distance at the supracellular level (Fig. 3F).

Taxonomic diversity does not covary with fungal disparity

With the evolution of fungal disparity characterised, we sought to understand its causality. To this end, we tested the link between fungal taxonomic diversity and disparity. We curated diversity data for each terminal in our dataset from the Catalogue of Life[23] and other sources[24-27]. We then mapped these diversity values across fungal phylomorphospace (Fig. 4A) and tested the strength of the relationship between morphological distance and pairwise differences in diversity

using the Mantel test (Fig. 4B). Neither approach presents a meaningful relationship between morphological disparity and taxonomic diversity.

Fungal disparity does not increase with genomic expansion

We tested whether genomic expansion, operationalised as increases in mean genome size and mean gene number, explains the radiation of fungi into new areas of morphospace. First, we curated mean genome size data from MycoCosm[28] and mapped it across fungal phylomorphospace, pruning out the terminals where molecular data were not available (Fig. 4C). We then tested for a correlation between the two using the Mantel test (Fig. 4D). Neither recover a compelling relationship between genome size and morphospace exploration. Similarly, mapping mean gene numbers across fungal phylomorphospace displays no discernible relationship between genomic expansion and morphospace occupation (Fig. 4E). Accordingly, this noncorrelation was borne out when the relationship between morphological distance and pairwise differences in mean gene number was assessed (Fig. 4F).

No early burst in the evolution of fungal disparity

In the context of analyses of disparity, the early burst model characterises the tendency for clades to maximise their phenotypic variance early in their evolutionary histories. To assess whether this model is compatible with the evolution of fungal disparity, we took time slices[29] of our tree from the mid-Tonian (~850 million years ago) to the present and used these to subsample the PCoA ordination of the main dataset. Our dataset does not include any fossil taxa. However, analyses of simulated and empirical data from animals have yielded meaningful insights into the evolution of disparity through time can be derived from extant data alone[6, 16]. In addition, we simulated 1000 datasets along our tree under an Mk model so that we could test whether patterns in fungal

disparity through time are explained by the Zero-Force Evolutionary Law (ZFEL), the null tendency for diversity to increase in evolutionary systems through time[20], once the null expectations of our phylogenetic sample are accounted for[16]. These simulated datasets were ordinated using PCoA and partitioned under the same scheme as the empirical data. We then characterised the size (Fig. 5) and density (Fig. 6) of the area of morphospace occupied by each of the empirical and simulated subsamples.

The sum of ranges of the empirical data spikes late in the Tonian, increases episodically until the end of the Permian, and then decreases until the present (Fig. 5A). This late Tonian spike is evident in the simulated datasets as well. However, post-Tonian the simulated datasets present a different pattern, as they exhibit a sustained increase in sum of ranges through time until the present. Except for a brief period in the Tonian, the sum of ranges of the empirical data consistently falls short of the null pattern presented by the simulated data. This contrasts with the patterns presented by the other two indices of size, the average Euclidean distance from centroid (Fig. 5B) and sum of variances (Fig. 5C), as both exceed the null expectation informed by the simulated data from the late Tonian onwards. These indices first deviate from the null pattern with a substantial spike during the late Tonian, continue to increase until the Permian, and then decrease to the present (Fig. 5B-C). In contrast, the simulated datasets exhibit an approximately gradual increase in sum of variances and average Euclidean distance from centroid through time, after an initial dip in the late Tonian.

The density with which fungi occupy empirical morphospace is more comparable to the null pattern of evolving morphospace occupation than the size of the area through time. When characterised using average nearest neighbour Euclidean distance and average minimum

spanning tree Euclidean distance, density displays an inverse relationship with size. The disparity of fungi within morphospace increases through time, rapidly and episodically at first but then at a lower rate average after the Tonian, up until the Permian. Thereafter, it increases approximately gradually until the present (Fig. 6A-B). The null expectation for fungal density through time is a gradual decrease from the late Tonian, regardless of the index employed. Where the empirical trends in density deviate from the null patterns depends on the index employed; when average nearest neighbour Euclidean distance is used (Fig. 6A), these deviations take the form of a sudden decrease during late Tonian, dips during late Ordovician–Permian, and an approximately gradual increase in density from the Triassic onwards. The average minimum spanning tree Euclidean distance presents a similar trend through time but differs in that between the Tonian and the Triassic, the density of the simulated datasets consistently exceeds that of the empirical data (Fig. 6B).

Discussion

In characterising and visualising the disparity of fungi, we have demonstrated that the distribution of fungal phenotypes is not determined by evolutionary convergence, despite the recurrence of specific phenotypic traits such as complex fruiting bodies[30]. Rather, the structure of fungal morphospace is defined by phenotypic divergence and consequently mirrors early taxonomic classifications based on morphology; historically, all flagellated, zygomycetous, sac-bearing, and club-bearing forms were united within the Chytridiomycota, Zygomycota, Ascomycota, and Basidiomycota respectively[31]. Therefore, it is unsurprising that they occupy distinct areas of morphospace. Within each morphotype, fungi are similarly divergent, as there is limited crossover of phylogenetic branches within the areas of phylomorphospace populated by

flagellated, zygomycetous, sac-bearing, and club-bearing forms. The difference in disparity between Dikarya and all other fungi is rooted in cellular and supracellular features. This is to be expected, given how unique dikaryotic multicellular organisation is within Fungi[8, 32]; within the kingdom, only Neolectomycetes, Pezizomycotina, and Agaricomycotina possess the ability to coordinate different cell types to form tissues[8, 30, 33]. Consequently, these dikarya have the broadest range of theoretically possible phenotypes amongst fungi. However, the overall distribution of fungal form is defined by subcellular features, which likely reflects the utility of the such characters in analyses of phylogeny[13]. This suggests that the structure of fungal morphospace has a strong phylogenetic component.

Phylogenetic intermediates bridge the gaps between occupied areas of fungal morphospace. Put another way, the clumpy distribution of fungi appears to be a product of the extinction of unrecorded intermediate phenotypes, which is plausible given the paucity of the fungal fossil record[19]. This result echoes that of broad scale analyses of animal disparity[6], as does the rate at which this distribution was achieved. Both our phylomorphospace and disparity through time analyses demonstrate that fungal phenotypic evolution is incompatible with the early burst/ maximal initial disparity model[5, 34, 35]. Instead, we find that the evolution of fungal morphospace is characterized by cumulative episodic increases over time, punctuated especially by the rapid expansion in phenotypic disparity associated with the emergence of multicellular zygomycetous taxa from their unicellular ancestors. This adds to the growing body of evidence that the early burst model is incompatible with the evolution of phenotypic diversity at the highest taxonomic levels[6].

Comparing our results to null expectations informed by simulated data, fungal disparity cannot be explained solely by the zero-force evolutionary law. The differences between the empirical and simulated datasets can be rationalised as a reflection of the hierarchical contingencies mapped across the former, which reflect biological reality. These contingencies allow us to differentiate between the absence of traits that are theoretically possible (i.e. true absences) and those that are impossible (i.e. inapplicable characters). A consequence of this coding scheme is that changes to the scoring of some characters will have a greater impact than others; the absence of key traits on which numerous other features are contingent upon is reflected across more characters than the absence of isolated traits, regardless of whether the contingent features themselves are present. In our dataset, these key traits are mostly synapomorphies and symplesiomorphies (e.g. presence of a zygospore, or an ascus, etc). Consequently, large numbers of taxa are differentiated from one another by entire suites of characters, which increases their overall spread in morphospace; the aspect of disparity characterised by sum of variances and average Euclidean distance from the centroid. Conversely, the absence of hierarchical contingency in the simulated data means that all character score combinations are possible. As such, the maximum possible difference between phenotypes is higher in our contingency-free simulations than in the empirical data, which is reflected in the greater sum of ranges of the simulated dataset. Taken together, these results suggest that hierarchical contingency promotes the evolution of greater phenotypic variance at the expense of a more constrained range.

Our analyses suggest that differences in genome size, the number of genes, and species-level diversity have little explanatory power when it comes to the evolution of fungal phenotypic variety. In contrast, differences in both species-level diversity and genome size correlate with phenotypic distance in animals when sampled at comparable taxonomic levels[6]. This decoupling

of diversity and disparity is not unique to fungi within Opisthokonta; many lower-rank metazoan clades show the same non-relationship[36-39]. Where our results do align with kingdom-wide analyses of animal disparity is in the correlation both present between organismal complexity and disparity[6]. These products of evolution are often linked and occasionally conflated[20]. However, instances in which the two are synonymised typically emerge from the implementation of outdated concepts of disparity and complexity[40]. Contemporary research continues to move towards more nuanced, descriptive characterisations of the distribution of organismal form, and away from rhetorical characterizations of "disparity"[40, 41]. In stark contrast, what constitutes organismal complexity lacks the same conceptual clarity, as it is used variably to quantify the traits that specify a phenotype[42], genetically uncorrelated phenotypic traits that contribute to an organism's fitness[43], cell types[44, 45], parts[20], and levels of organisation[20], as well as the presence of multicellularity[46]. Mycological definitions typically align with the latter, equating complexity to the presence of multicellular fruiting bodies[8, 30, 32], although this is sometimes expanded to a coarse categorical scale that also encompasses unicellularity, hyphal organisation, and mycelial growth[32].

While our definition differs from the mycological norm, the result is the same; increases in fungal complexity through time predominantly reflect the diversification and elaboration of multicellular phenotypes. Just as phenotypic disparity has evolved episodically within Fungi, so too has complexity. The most notable episode occurs with the emergence of Dikarya, an event that coincides with the evolution of multicellular fruiting bodies[32] – the most complex structures in the fungal kingdom[8, 30]. The phenotypic diversification of Dikarya can be attributed to the evolution of these fruiting bodies, as the presence of these structures expands the range of possible phenotypes considerably. However, our analyses demonstrate that subcellular

phenotypic traits define the overall distribution of fungi in morphospace, despite the weak correlation between complexity and disparity they present. Consequently, changes in fungal complexity cannot be invoked as the sole driver of broader patterns in fungal disparity. This is an apt demonstration of how these concepts are linked but not interchangeable; an evolutionary increase in the number of parts within members of a clade (complexity) does not always yield an increase in the phenotypic variation between them (disparity).

At the highest taxonomic levels, both animals and fungi exhibit an episodic increase in disparity through time, yielding a continuous distribution of phenotypic variety made patchy by the subsequent extinction and non-preservation of phylogenetic intermediates[6]. This suggests a commonality in the mode with which multicellular body plans diversify. The reported tendency for animal clades to maximise their phenotypic variety relatively early in their evolutionary histories appears restricted to lower taxonomic levels. Whether this result reflects a general evolutionary phenomenon, an indicator that such patterns are unique to specific lineages, or an artefact of sampling, is unclear. What is clear is that the early burst model is not compatible with patterns in phenotypic evolution at the broadest of scales.

In conclusion, our results demonstrate that fungal phenotypic disparity has increased episodically through time, with the discontinuous distribution of extant forms likely a product of the extinction of unobserved phylogenetic intermediates. The similarity of these patterns to those presented by animals suggests a common evolutionary mode at the highest taxonomic levels within Opisthokonta. Unlike animals, fungal species-level diversity, genome size, and gene number offer little explanation for observed patterns in phenotypic disparity. Additionally, the ZFEL alone cannot explain the patterns we recover. Like phenotypic disparity, fungal complexity

has evolved episodically, with the evolution of multicellular fruiting bodies producing the most substantial step change. Increases in multicellular complexity explain the phenotypic diversification of dikaryotic fungi but offer little explanation for the overall structure of fungal morphospace, which appears to be rooted in differences in subcellular phenotype. These patterns mirror the evolution of phenotypic disparity in animals, suggesting that organismal grade multicellular body plans may evolve through a common process.

Methods

Data collection

Phenotypic character data was sourced from the AFTOL database[14] and the wider literature (for a full list of sources, see Supplemental Information). Taxon sampling was informed by cross-referencing a recent review of fungal diversity[13] with the taxonomic coverage of the AFTOL database[14], which represents the limit of our understanding of subcellular phenotypic variation in fungi. This provided the best compromise between phenotypic data availability and representative sampling of fungal diversity, although considerable taxonomic rank heterogeneity was introduced as a result; the final dataset included 2 phyla, 3 subphyla, 29 classes, 8 orders, 1 family, and 1 genus. In total, the dataset was comprised of 303 characters scored for 44 taxa. Characters capturing phenotypic traits at the subcellular level were categorised as such; all other characters were designated as “supracellular”. Using this categorisation, subcellular and supracellular subsets were derived from the main dataset.

For each of these subsets and the main dataset, accompanying complexity data were derived by summing the character scores for each taxon. States scored as inapplicable (“-“) were treated as

absent (“0”) in these calculations. Complementary diversity data for each taxon were from the Catalogue of Life[47] and the literature[24-27]. Complementary molecular data were obtained from Mycocosm[28] by averaging the genome size and gene number values for the constituent species of each taxon in our dataset.

Ancestral state estimation

Ancestral state estimation (ASE) requires a time-calibrated tree matching the taxon content of the dataset being analysed. To this end, the tree included in the review that informed dataset assembly[13] was pruned to match the taxon sampling of the character data. The topology was updated using recent molecular analyses for reference[10] and coarsely time-calibrated using the tree.age function included in the dispRity R package[48] and a root age estimate of 1042 million years[49]. These calibrations were then refined using previously-published divergence time estimates to ensure key nodes were dated as accurately as possible[49-51].

Ancestral states were estimated for each node using stochastic character mapping [52] via the phytools make.simmap function[53]. 1000 simulations were conducted under an equal-rates model. Each character was scored for each node using a probability threshold of 0.5; characters were scored as missing (“?”) if none of the posterior probabilities of the possible states met or exceeded the threshold. The estimated states for each character were added to both the main empirical dataset and the relevant subset.

Data simulation

Binary character data were simulated along the tree using the protocol and scripts of Smith et al.[16]. 1000 matrices of 303 characters were simulated under an equal-rates model, where the rates

were set as the mean of 1000 samples from a gamma distribution with *shape* = 0.44 and *rate* = the sum of all branch lengths of the tree. Each character was simulated independently and states were recorded for all nodes and tips in the tree. Matrices with unrealistically high levels of homoplasy, defined as consistency index values greater than 0.259[54, 55], were discarded and replaced.

Distance matrix computation

To permit distance matrix computation, the empirical datasets were recoded so that states originally scored as inapplicable ("-") were changed to "0", and all other state scores were increased by 1. For each empirical and simulated dataset, a 44 x 44 (the number of taxa in the dataset) pairwise distance matrix was derived using the Claddis calculate_morphological_distances function[56] to calculate the Gower dissimilarity coefficient[57] for each pair of taxa. This coefficient accommodates missing data better than other distance metrics[58]. In preparation for ordination, the resulting Gower coefficients were transformed through application of a square root term to make the distances approximately Euclidean[59].

Ordination

The empirical distance matrices were ordinated in two ways: non-metric multidimensional scaling (NMDS) using the vegan metaMDS function, and principal coordinates analysis (PCoA/PCA), sometimes referred to as classical multidimensional scaling, using the ape pcoa function [60]. The simulated distance matrices were only ordinated using PCoA, as we only sought to quantitatively characterise their disparity.

Multiple rounds of NMDS were conducted to identify the lowest K value (i.e. the number of dimensions) that captured the distribution of taxa in morphospace in a representative way. While this determination is somewhat subjective, stress values, measures of the fit of the variation in a dataset to the number of dimensions prescribed, of less than 0.2 generally indicate that the resulting ordination is a good representation of the data[61]. For the main empirical dataset and both subsets, the NMDS ordinations conducted with K = 2 returned stress values markedly below 0.2 (Figs S1-S3). While the K = 3 stress values were lower than the K = 2, the difference was minor compared to the drop in stress from K = 1 to K = 2. This indicated that two-dimensional NMDS provided the best compromise between preserving the structure of the variation in our data and minimising the dimensionality of the resulting ordination for more intuitive visualisation. As such, all NMDS ordinations of our data were conducted with the number of dimensions set to two.

Prior to PCoA, the Cailliez correction[62] was applied to the Gower coefficient values of all distance matrices to protect against the potential issue of negative eigenvalues. These were then ordinated using PCoA. The two outgroup taxa (Fonticulida and Nucleariida) were removed from the resulting ordinations as they do not contribute to fungal disparity.

For the empirical PCoA ordinations, we sought to identify the number of dimensions that characterised the distribution of fungal phenotypes in the most comparable way to the NMDS ordinations. From the empirical PCoA outputs, partitions were derived that included axes 1–2, 1–3, 1–4, and so forth, with the final partition including all PCoA axes. 1000 subsamples of 21 taxa (50% of the original ordination) were then taken from each of these partitions and their disparity was characterised using five indices (see below for a description of each). The same subsampling procedure was applied to the NMDS ordination to generate a comparable set of subsamples, the

disparity of which were characterised using the same five indices. Spearman's rank correlation coefficient was then used to test the relationship between the disparity of the NMDS subsamples and that of the subsamples of each PCoA partitions across all five indices. The strength of the resulting correlation coefficients indicated that the first five, six, and 4 axes of the empirical PCoA ordinations of the main dataset, subcellular subset, and supracellular subset respectively provided the best approximation of the distributions characterised by the equivalent NMDS ordinations. These sets of axes represented the majority of the eigenvalues produced by their respective PCoAs (Figs S4-S6), which indicated that they captured the bulk of the variation present for all three variants of our dataset. Therefore, we characterise empirical fungal disparity using these sets of PCoA axes for the main dataset and each subset to maximise compatability between the outputs of the two ordination methods we employ.

Characterising phenotypic disparity

Five indices were used to characterise fungal disparity across all analyses of the PCoA ordinations: sum of ranges, average Euclidean distance from centroid, sum of variances, average nearest neighbour distance, and minimum spanning tree average distance. These indices were calculated using the relevant functions in the dispRity package[48]. Each index characterises different aspects of morphospace occupation but can be coarsely divided into indices of size (sum of ranges, sum of variances, average Euclidean distance from centroid) and density (average nearest neighbour distance, minimum spanning tree average distance). Sum of variances is traditionally considered an index of size but can fluctuate with changes in density in normally distributed morphospaces. However, as such morphospaces are rare, it is most informative when employed as an index of size[16]. Simulation studies have shown sum of variances and average Euclidean distance from centroid to be reliable descriptors of the size of an area of occupied

morphospace, just as average nearest neighbour distance and minimum spanning tree average distance are for the density with which taxa occupy a region[41]. Sum of ranges was added to this repertoire of proven indices as it characterises a different aspect of the size of an occupied area to the other indices; rather than the overall spread of a point cloud, it measures the divergence of peripheral phenotypes[16]. These indices were used to characterise the morphospace occupation of 1000 bootstraps of the four fungal morphotypes identified in our analyses, as well as all dikaryotic and non-dikaryotic fungi.

Disparity through time

Time slicing[29] was conducted under the "proximity" model using the dispRity chrono.subsets function [48] to derive subsamples of the empirical and simulated PCoA ordinations at different stages in the history of Fungi. Samples were taken during the Proterozoic at the boundaries between the Stenian, Tonian, Cryogenian, and Ediacaran periods and every 10 million years in between. During the Phanerozoic, samples were taken at the boundaries of every stratigraphic age.

Each empirical time subsample was bootstrapped 100 times, with the size of the bootstrap set to three. The disparity of each of these bootstraps was characterised using all five indices, generating 100 values of each index for each time subsample. These values were summarised through derivation of the median, 5% quantile, and 95% quantile values for each time subsample. For each time subsample of each simulated matrix, the same bootstrapping and disparity characterisation procedure was applied. This produced 1000 median, 5% quantile, and 95% quantile values for each time subsample. These values were then summarised themselves in the same fashion; through identification of the median and 5% and 95% quantile values.

Disparity versus potentially explanatory variables

To match the pairwise distances matrices already calculated using the Gower coefficient, the pairwise differences in complexity were derived for the main dataset and both subsets for each taxon pair. Pairwise differences in diversity, genome size, and genome length were also calculated for each taxon pair. These were arranged as pairwise difference matrices to match the structure of those characterising phenotypic distance. This allowed us to test for correlation between the two using the Mantel test. As molecular data were not available for Entorrhizomycotina, Cryptomycocolacomycetes, Laboulbeniomycetes, and Lichinomycetes, taxon pairs including these taxa were omitted from the analyses testing for correlation between disparity, genome size, and gene number.

Data availability

All original data (empirical and simulated) used in this study have been deposited at Dryad[63] and are publicly available at https://doi.org/10.5061/dryad.wwpzgmsm9.

Code availability

All code used in this study has been deposited at Dryad[63] and is publicly available at https://doi.org/10.5061/dryad.wwpzgmsm9.

Acknowledgements

We thank Gary Storey, Anna Larkin, Donna Rainey, Rebecca Wheeler, and all the other Twitter users who kindly provided photographs of fungi for consideration for inclusion in this paper. We

would also like to thank Pedro Godoy and one other anonymous referee for their thoughtful comments during the review process, as the manuscript was much improved for their input. TJS was funded by a Natural Environment Research Council (NERC) PhD Studentship within the GW4+ Doctoral Training Programme. PCJD was funded by the Natural Environment Research Council (NE/P013678/1; part of the Biosphere Evolution, Transitions and Resilience (BETR) programme, co-funded by the Natural Science Foundation of China (NSFC)); the Biotechnology and Biological Sciences Research Council (BB/T012773/1; BB/N000919/1); the Gordon and Betty Moore Foundation (GBMF9741); the John Templeton Foundation (Grant 62220; the opinions expressed in this publication are those of the authors and do not necessarily reflect the views of the John Templeton Foundation) and the Leverhulme Trust (RF-2022-167).

Author contributions

Both authors contributed to the conceptualisation and design of the study, its component experiments, and the interpretation of the results. TJS collected the data, conducted the analyses, and drafted the manuscript, to which PCJD contributed.

Competing interests

The authors declare no competing interests.

Figure legends

Figure 1. The evolutionary interrelationships of the nine major fungal lineages. (A) *Rozella rhizoclosmatii* zoospore from[64]. (B) *Rozella allomycetis* resting spores (labelled Sp) within parasitized hyphae (labelled H) of *Allomyces macrogynus* from[64]. (C) *Allomyces moniliformis*

sporangia from[65]. (D) *Zygorhizidium willei* developing sporangium from[66]. (E) *Liebetanzomyces polymorphus* sporangium and rhizoids from[67]. (F) *Glomus atlanticum* spores in cluster from[68].(G) *Rhizomucor pusillus* sporangiophores from[69]. (H) *Piptocephalis* sp. (Zoopagomycota) zygospore from[70]. (I) *Piptocephalis cylindrospora* (Zoopagomycota) sporangiophores from[70]. (J) *Russula sanguinaria* fruiting body (photo by Gary Storey). (K) *Grifola frondose* fruiting body (photo by Anna Larkin). (L) *Hypocreopsis rhododendri* fruiting body (photo by Donna Rainey). (M) *Cordyceps militaris* fruiting bodies (photo by Rebecca Wheeler). Node 1 = last fungal common ancestor (LFCA), Node 2 = Chytridiomyceta, Node 3 = Dikarya.

Figure 2. The distribution of fungi in morphospace. (A) An NMDS phylomorphospace of fungi. (B) The sum of ranges and average minimum spanning tree Euclidean distance of 1000 bootstraps of the four fungal morphotypes (flagellated, zygomycetous, sac, club), Dikarya, and non-dikaryotic fungi. (C) A subcellular NMDS phylomorphospace of fungi. (D) The subcellular sum of ranges, average nearest neighbour (NN) Euclidean distance, and average minimum spanning tree Euclidean distance of 1000 bootstraps of the four fungal morphotypes (flagellated, zygomycetous, sac, club), Dikarya, and non-dikaryotic fungi. (E) A subcellular NMDS phylomorphospace of fungi. (F) The subcellular sum of ranges and average minimum spanning tree Euclidean distance of 1000 bootstraps the four fungal morphotypes (flagellated, zygomycetous, sac, club), Dikarya, and non-dikaryotic fungi. Box plot whiskers extend to minima and maxima of data; boxes capture interquartile range and median.

Figure 3. The relationship between phenotypic disparity and organismal complexity in fungi. (A) An NMDS phylomorphospace of fungi where point size scales with complexity. (B) The relationship between Gower coefficient (i.e. pairwise phenotypic distance) and pairwise

differences in complexity for all characters. (C) A subcellular NMDS phylomorphospace of fungi where point size scales with complexity. (D) The relationship between Gower coefficient and pairwise differences in complexity for subcellular characters only. (E) A supracellular NMDS phylomorphospace of fungi where point size scales with complexity. (D) The relationship between Gower coefficient and pairwise differences in complexity for supracellular characters only. Complexity was scaled to a range of 0-2 prior to plotting. How disparity correlated with complexity was assessed using the Mantel test.

Figure 4. How phenotypic disparity relates to taxonomic diversity, genome size, and gene number in fungi. (A) An NMDS phylomorphospace of fungi where point size scales with taxonomic diversity. (B) The relationship between Gower coefficient (i.e. pairwise phenotypic distance) and logarithmically transformed pairwise differences in taxonomic diversity for all characters. (C) An NMDS phylomorphospace of fungi where point size scales with average genome size. (D) The relationship between Gower coefficient and logarithmically transformed pairwise differences in average genome size. (E) An NMDS phylomorphospace of fungi where point size scales with average gene number. (F) The relationship between Gower coefficient and logarithmically transformed pairwise differences in average gene number. Prior to plotting, taxonomic diversity, average genome size, and average gene number were rescaled to a range of 0-2. How disparity correlated with diversity, genome size, and gene number was assessed using the Mantel test.

Figure 5. Changes in the size of the area of morphospace occupied by fungi through time. (A) Fungal sum of ranges through time. (B) Fungal average Euclidean distance from centroid through time. (C) Fungal sum of variances through time. In each panel, empirical trends in fungal

disparity through time (solid lines) are plotted against the null expectation of random evolution given our phylogenetic sample of fungal diversity (dashed line). Both the solid and dashed lines represent median values; the former of the empirical bootstraps, the latter of the bootstraps of the simulated matrices comprising the null expectation. The shaded area represents the 90% confidence interval of the null expectation.

Figure 6. Changes in the density with which fungi occupy morphospace through time. (A) Fungal average nearest neighbour Euclidean distance through time. (B) Fungal average minimum spanning tree Euclidean distance through time. In each panel, empirical trends in fungal disparity through time (solid lines) are plotted against the null expectation of random evolution given our phylogenetic sample of fungal diversity (dashed line). Both the solid and dashed lines represent median values; the former of the empirical bootstraps, the latter of the bootstraps of the simulated matrices comprising the null expectation. The shaded area represents the 90% confidence interval of the null expectation.

References

1. Niklas, K.J. & Newman, S.A. The many roads to and from multicellularity. *J. Exp. Bot.* **71**, 3247-3253 (2020).
2. Maynard Smith, J. & Szathmary, E. *The major transitions in evolution*. (W. H. Freeman Spektrum, Oxford, New York; 1995).
3. Grosberg, R.K. & Strathmann, R.R. The evolution of multicellularity: a minor major transition?, in *Annual Review of Ecology Evolution and Systematics*, Vol. 38 621-654 (Annual Reviews, Palo Alto; 2007).

4. Erwin, D.H. Disparity: Morphological pattern and developmental context. *Palaeontology* **50**, 57-73 (2007).
5. Foote, M. The evolution of morphological diversity. *Annu. Rev. Ecol. Syst.* **28**, 129-152 (1997).
6. Deline, B. *et al.* Evolution of metazoan morphological disparity. *Proceedings of the National Academy of Sciences of the United States of America* **115**, E8909-E8918 (2018).
7. Hughes, M., Gerber, S. & Wills, M.A. Clades reach highest morphological disparity early in their evolution. *Proceedings of the National Academy of Sciences of the United States of America* **110**, 13875-13879 (2013).
8. Kues, U., Khonsuntia, W. & Subba, S. Complex fungi. *Fungal Biol. Rev.* **32**, 205-218 (2018).
9. Blackwell, M. The Fungi: 1, 2, 3 … 5.1 million species? *American Journal of Botany* **98**, 426-438 (2011).
10. Li, Y. *et al.* A genome-scale phylogeny of the kingdom Fungi. *Current Biology* **31**, 1653-1665.e1655 (2021).
11. Chang, Y. *et al.* Genome-scale phylogenetic analyses confirm Olpidium as the closest living zoosporic fungus to the non-flagellated, terrestrial fungi. *Scientific Reports* **11**, 12 (2021).
12. James, T.Y., Stajich, J.E., Hittinger, C.T. & Rokas, A. Toward a fully resolved fungal tree of life, in *Annual Review of Microbiology, Vol 74, 2020*, Vol. 74. (ed. S. Gottesman) 291-313 (Annual Reviews, Palo Alto; 2020).
13. Naranjo-Ortiz, M.A. & Gabald?n, T. Fungal evolution: diversity, taxonomy and phylogeny of the Fungi. *Biol. Rev.* **94**, 2101-2137 (2019).

14. Celio, G.J., Padamsee, M., Dentinger, B.T.M., Bauer, R. & McLaughlin, D.J. Assembling the fungal tree of life: constructing the structural and biochemical database. *Mycologia* **98**, 850-859 (2006).
15. Gerber, S. Use and misuse of discrete character data for morphospace and disparity analyses. *Palaeontology* **62**, 305-319 (2019).
16. Smith, T.J., Puttick, M.N., O'Reilly, J.E., Pisani, D. & Donoghue, P.C.J. Phylogenetic sampling affects evolutionary patterns of morphological disparity. *Palaeontology* (2021).
17. Adl, S.M. *et al.* Revisions to the classification, nomenclature, and diversity of eukaryotes. *J. Eukaryot. Microbiol.* **66**, 4-119 (2019).
18. Berbee, M.L. *et al.* Genomic and fossil windows into the secret lives of the most ancient fungi. *Nat. Rev. Microbiol.* **18**, 717-730 (2020).
19. Taylor, T.N., Krings, M. & Taylor, E. *Fossil Fungi*. (Elsevier, 2015).
20. McShea, D.W. & Brandon, R.N. *Biology's First Law: The Tendency for Diversity and Complexity to Increase in Evolutionary Systems*. (University of Chicago Press, Chicago, USA; 2010).
21. McShea, D.W. Metazoan complexity and evolution: is there a trend? *Evolution* **50**, 477-492 (1996).
22. Ispolatov, I., Alekseeva, E. & Doebeli, M. Competition-driven evolution of organismal complexity. *PLoS Comput. Biol.* **15**, 16 (2019).
23. Bánki, O. *et al.* Catalogue of Life checklist (Version 2021-08-25). (2021).
24. Bauer, R. *et al.* Entorrhizomycota: a new fungal phylum reveals new perspectives on the evolution of Fungi. *Plos One* **10**, 19 (2015).
25. Jones, M.D.M. *et al.* Discovery of novel intermediate forms redefines the fungal tree of life. *Nature* **474**, 200-U234 (2011).

26. Yoshida, M., Nakayama, T. & Inouye, I. *Nuclearia thermophila* sp nov (Nucleariidae), a new nucleariid species isolated from Yunoko Lake in Nikko (Japan). *Eur. J. Protistol.* **45**, 147-155 (2009).
27. Hibbett, D.S. *et al.* A higher-level phylogenetic classification of the Fungi. *Mycol. Res.* **111**, 509-547 (2007).
28. Grigoriev, I.V. *et al.* MycoCosm portal: gearing up for 1000 fungal genomes. *Nucleic Acids Res.* **42**, D699-D704 (2014).
29. Guillerme, T. & Cooper, N. Time for a rethink: time sub-sampling methods indisparity-through-time analyses. *Palaeontology* **61**, 481-493 (2018).
30. Nagy, L.G., Kovacs, G.M. & Krizsan, K. Complex multicellularity in fungi: evolutionary convergence, single origin, or both? *Biol. Rev.* **93**, 1778-1794 (2018).
31. Whittaker, R.H. New concepts of kingdoms of organisms. *Science* **163**, 150-+ (1969).
32. Naranjo-Ortiz, M.A. & Gabaldon, T. Fungal evolution: cellular, genomic and metabolic complexity. *Biol. Rev.* **95**, 1198-1232 (2020).
33. Nguyen, T.A. *et al.* Innovation and constraint leading to complex multicellularity in the Ascomycota. *Nat. Commun.* **8**, 13 (2017).
34. Briggs, D.E.G., Fortey, R.A. & Wills, M.A. Morphological disparity in the Cambrian. *Science* **256**, 1670-1673 (1992).
35. Gould, S.J. *Wonderful Life: The Burgess Shale and the Nature of History*. (Huchinson Radius, London, UK; 1990).
36. Wan, J.Y. *et al.* Decoupling of morphological disparity and taxonomic diversity during the end-Permian mass extinction. *Paleobiology* **47**, 402-417 (2021).

37. Grossnickle, D.M. & Newham, E. Therian mammals experience an ecomorphological radiation during the Late Cretaceous and selective extinction at the K-Pg boundary. *Proc. R. Soc. B-Biol. Sci.* **283**, 8 (2016).

38. Ruta, M., Angielczyk, K.D., Frobisch, J. & Benton, M.J. Decoupling of morphological disparity and taxic diversity during the adaptive radiation of anomodont therapsids. *Proc. R. Soc. B-Biol. Sci.* **280**, 9 (2013).

39. Bapst, D.W., Bullock, P.C., Melchin, M.J., Sheets, H.D. & Mitchell, C.E. Graptoloid diversity and disparity became decoupled during the Ordovician mass extinction. *Proceedings of the National Academy of Sciences of the United States of America* **109**, 3428-3433 (2012).

40. Guillerme, T. *et al.* Disparities in the analysis of morphological disparity. *Biol. Lett.* **16**, 8 (2020).

41. Guillerme, T., Puttick, M.N., Marcy, A.E. & Weisbacker, V. Shifting spaces: which disparity or dissimilarity measurement best summarize occupancy in multidimensional spaces? *Ecol. Evol.* **10**, 7261-7275 (2020).

42. Svardal, H., Rueffler, C. & Doebeli, M. Organismal complexity and the potential for evolutionary diversification. *Evolution* **68**, 3248-3259 (2014).

43. Tenaillon, O., Silander, O.K., Uzan, J.P. & Chao, L. Quantifying organismal complexity using a population genetic approach. *Plos One* **2**, 8 (2007).

44. Valentine, J.W., Collins, A.G. & Meyer, C.P. Morphological complexity increase in metazoans. *Paleobiology* **20**, 131-142 (1994).

45. Yang, J., Lusk, R. & Li, W.H. Organismal complexity, protein complexity, and gene duplicability. *Proceedings of the National Academy of Sciences of the United States of America* **100**, 15661-15665 (2003).

46. Prochnik, S.E. *et al.* Genomic analysis of organismal complexity in the multicellular green alga *Volvox carteri*. *Science* **329**, 223-226 (2010).
47. Hobern, D. *et al.* Towards a global list of accepted species VI: the Catalogue of Life checklist. *Organisms Diversity & Evolution* **21**, 677-690 (2021).
48. Guillerme, T. dispRity: A modular R package for measuring disparity. *Methods Ecol. Evol.* **9**, 1755-1763 (2018).
49. Tedersoo, L. *et al.* High-level classification of the Fungi and a tool for evolutionary ecological analyses. *Fungal Divers.* **90**, 135-159 (2018).
50. He, M.Q. *et al.* Notes, outline and divergence times of Basidiomycota. *Fungal Divers.* **99**, 105-367 (2019).
51. Beimforde, C. *et al.* Estimating the Phanerozoic history of the Ascomycota lineages: combining fossil and molecular data. *Mol. Phylogenet. Evol.* **78**, 386-398 (2014).
52. Bollback, J.P. SIMMAP: Stochastic character mapping of discrete traits on phylogenies. *BMC Bioinformatics* **7**, 7 (2006).
53. Revell, L.J. phytools: an R package for phylogenetic comparative biology (and other things). *Methods Ecol. Evol.* **3**, 217-223 (2012).
54. O'Reilly, J.E. *et al.* Bayesian methods outperform parsimony but at the expense of precision in the estimation of phylogeny from discrete morphological data. *Biol Lett* **12** (2016).
55. Sanderson, M.J. & Donoghue, M.J. Patterns of variation in levels of homoplasy. *Evolution* **43**, 1781-1795 (1989).
56. Lloyd, G.T. Estimating morphological diversity and tempo with discrete character-taxon matrices: implementation, challenges, progress, and future directions. *Biol. J. Linnean Soc.* **118**, 131-151 (2016).

57. Gower, J.C. General coefficient of similarity and some of its properties. *Biometrics* **27**, 857-& (1971).
58. Anderson, P.S.L. & Friedman, M. Using cladistic characters to predict functional variety: experiments using early gnathostomes. *J. Vertebr. Paleontol.* **32**, 1254-1270 (2012).
59. Wills, M.A. Morphological disparity: a primer, in *Fossils, phylogeny, and form: An analytical approach*. (eds. J.M. Adrain, G.D. Edgecombe & D.S. Lieberman) 55–144 (Springer, New York, USA; 2001).
60. Paradis, E. & Schliep, K. ape 5.0: an environment for modern phylogenetics and evolutionary analyses in R. *Bioinformatics* **35**, 526-528 (2019).
61. Clarke, K.R. & Warwick, R.M. *Change in Marine Communities: An Approach to Statistical Analysis and Interpretation*, Edn. 2nd. (PRIMER-E, Plymouth; 2001).
62. Cailliez, F. The analytical solution of the additive constant problem *Psychometrika* **48**, 305-308 (1983).
63. Smith, T.J. & Donoghue, P.C.J. Data from: Patterns and processes in the evolution of fungal phenotypic disparity. *Dryad* (2022).
64. Letcher, P.M. & Powell, M.J. A taxonomic summary and revision of *Rozella* (Cryptomycota). *IMA Fungus* **9**, 383-399 (2018).
65. James, T., Porter, T.M. & Martin, W.W. 7 Blastocladiomycota, in *Systematics and Evolution. The Mycota (A Comprehensive Treatise on Fungi as Experimental Systems for Basic and Applied Research)*, Vol. 7A. (eds. D.J. McLaughlin & J.W. Spatafora) (Springer, Berlin, Heidelberg; 2014).
66. Seto, K., Van den Wyngaert, S., Degawa, Y. & Kagami, M. Taxonomic revision of the genus *Zygorhizidium*: Zygorhizidiales and Zygophlyctidales ord. nov. (Chytridiomycetes, Chytridiomycota). *Fungal Systematics and Evolution* **5**, 17-38 (2020).

67. Joshi, A. *et al.* Liebetanzomyces polymorphus gen. et sp nov., a new anaerobic fungus (Neocallimastigomycota) isolated from the rumen of a goat. *MycoKeys*, 89-110 (2018).
68. Blaszkowski, J. *et al.* Dominikia bonfanteae and Glomus atlanticum, two new species in the Glomeraceae (phylum Glomeromycota) with molecular phylogenies reconstructed from two unlinked loci. *Mycol. Prog.* **20**, 131-148 (2021).
69. Walther, G., Wagner, L. & Kurzai, O. Outbreaks of Mucorales and the species involved. *Mycopathologia* **185**, 765-781 (2020).
70. Reynolds, N.K. *et al.* Phylogenetic and morphological analyses of the mycoparasitic genus Piptocephalis. *Mycologia* **111**, 54-68 (2019).

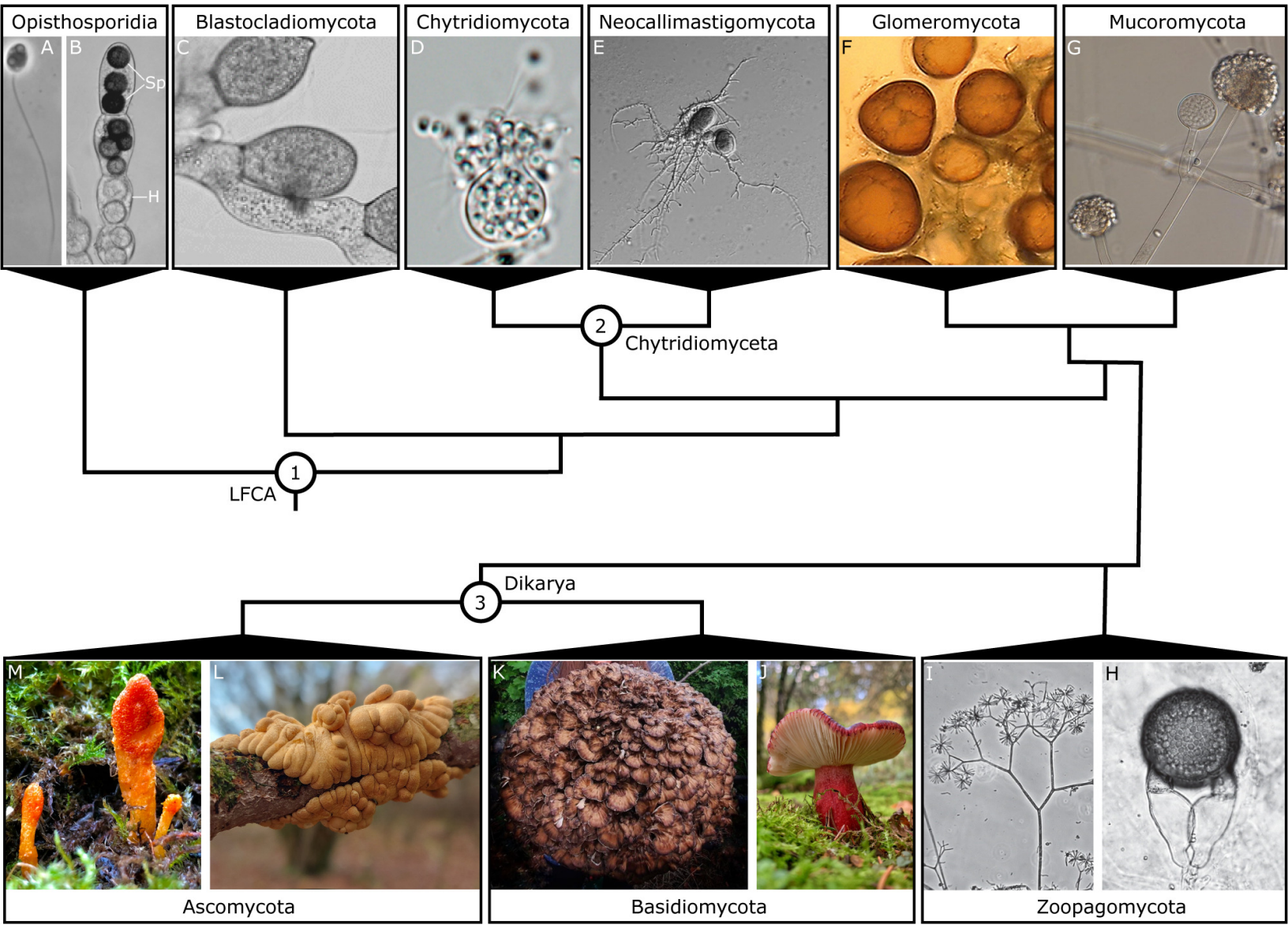
Opisthosporidia
A
B
Sp
H
Blastocladiomycota
C
Chytridiomycota
D
Neocallimastigomycota
E
Glomeromycota
F
Mucoromycota
G
2
Chytridiomyceta
1
LFCA
3
Dikarya
M
L
K
J
I
H
Ascomycota
Basidiomycota
Zoopagomycota

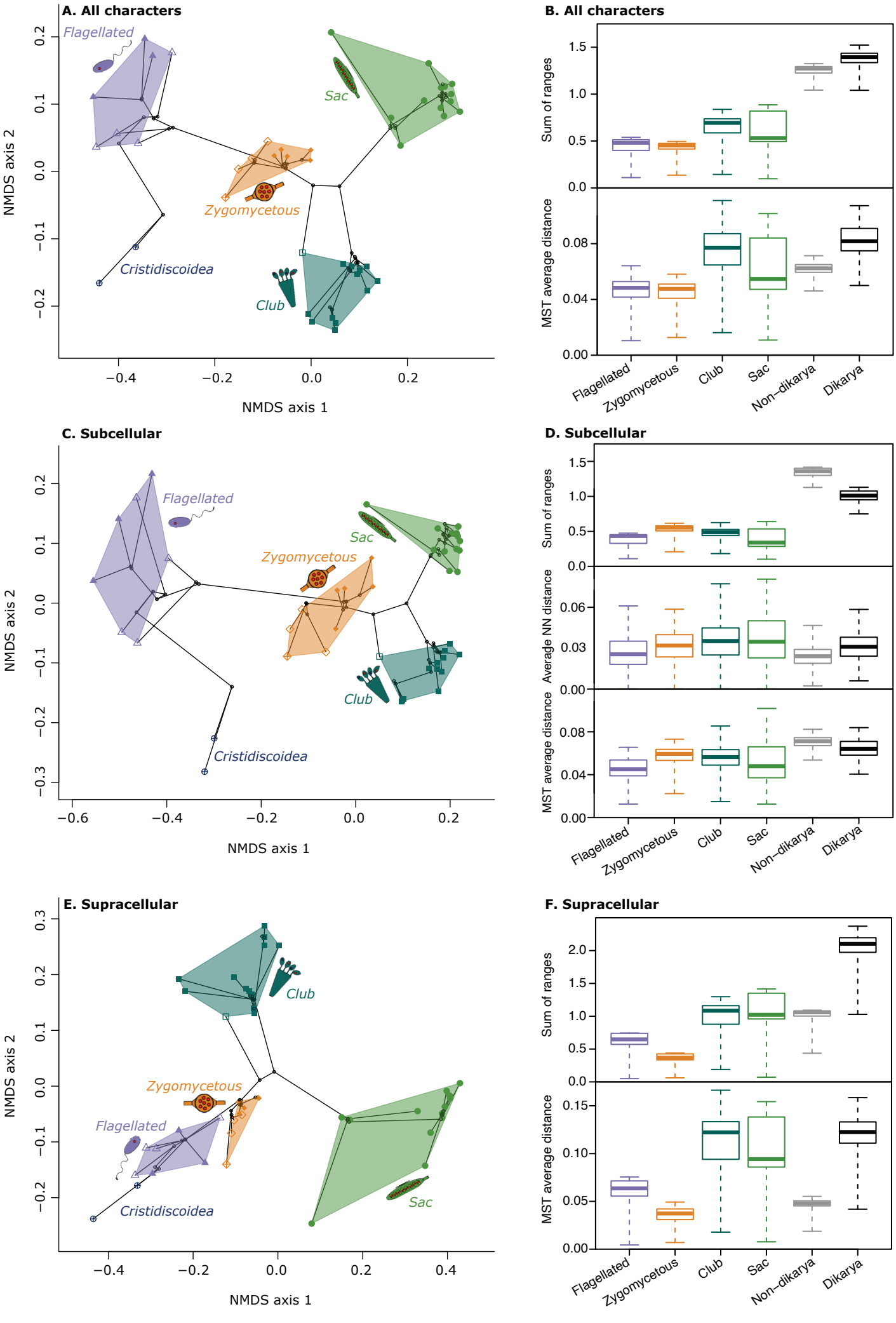
A. All characters
Flagellated
Sac
Zygomycetous
Cristidiscoidea
Club
NMDS axis 2
NMDS axis 1
B. All characters
Sum of ranges
MST average distance
Flagellated
Zygomycetous
Club
Sac
Non–dikarya
Dikarya
C. Subcellular
D. Subcellular
Average NN distance
E. Supracellular
F. Supracellular

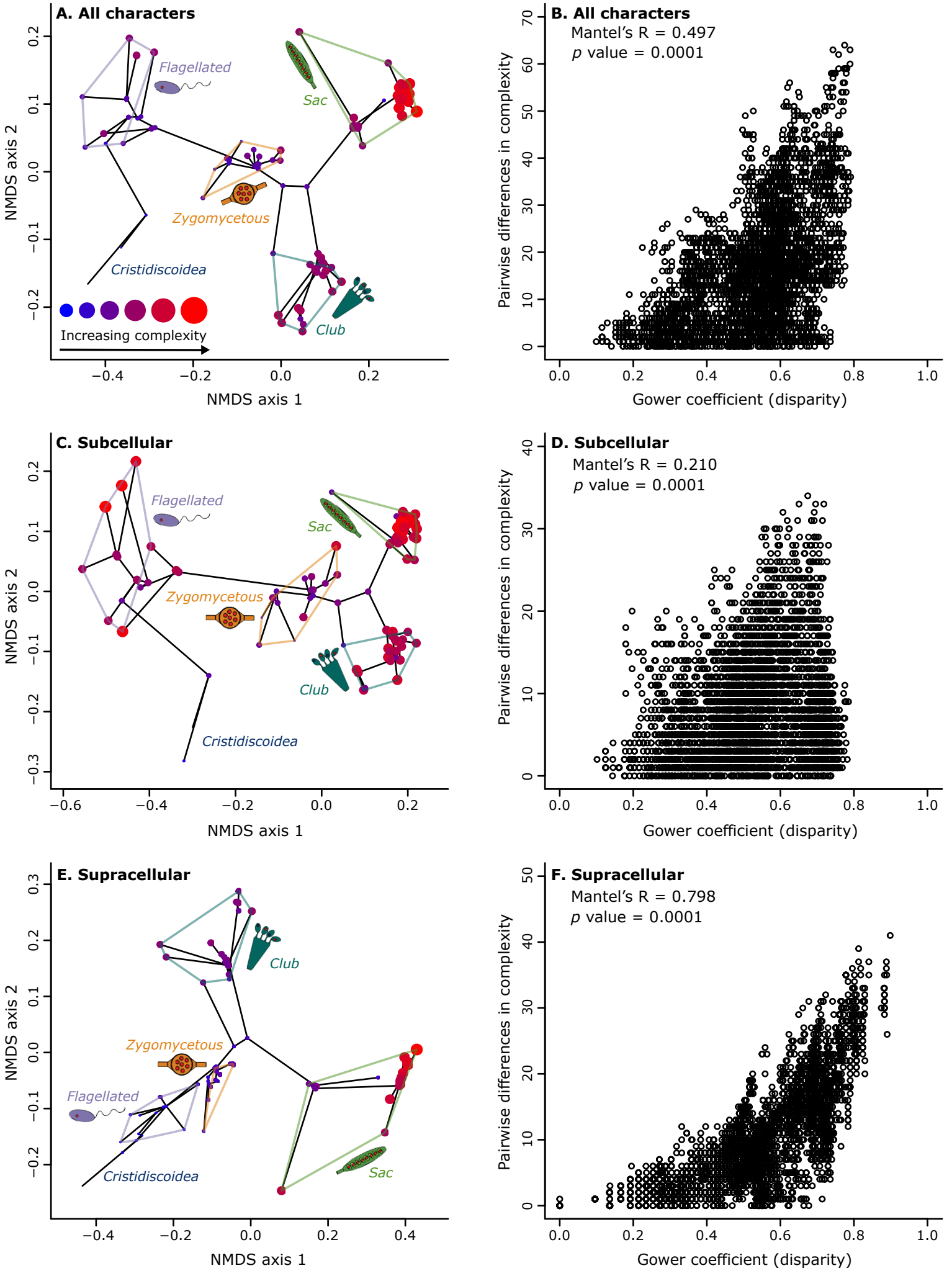
A. All characters
Flagellated
Sac
Zygomycetous
Cristidiscoidea
Club
Increasing complexity
NMDS axis 2
NMDS axis 1
B. All characters
Mantel's R = 0.497
p value = 0.0001
Pairwise differences in complexity
Gower coefficient (disparity)
C. Subcellular
Flagellated
Sac
Zygomycetous
Club
Cristidiscoidea
NMDS axis 2
NMDS axis 1
D. Subcellular
Mantel's R = 0.210
p value = 0.0001
Pairwise differences in complexity
Gower coefficient (disparity)
E. Supracellular
Club
Zygomycetous
Flagellated
Cristidiscoidea
Sac
NMDS axis 2
NMDS axis 1
F. Supracellular
Mantel's R = 0.798
p value = 0.0001
Pairwise differences in complexity
Gower coefficient (disparity)

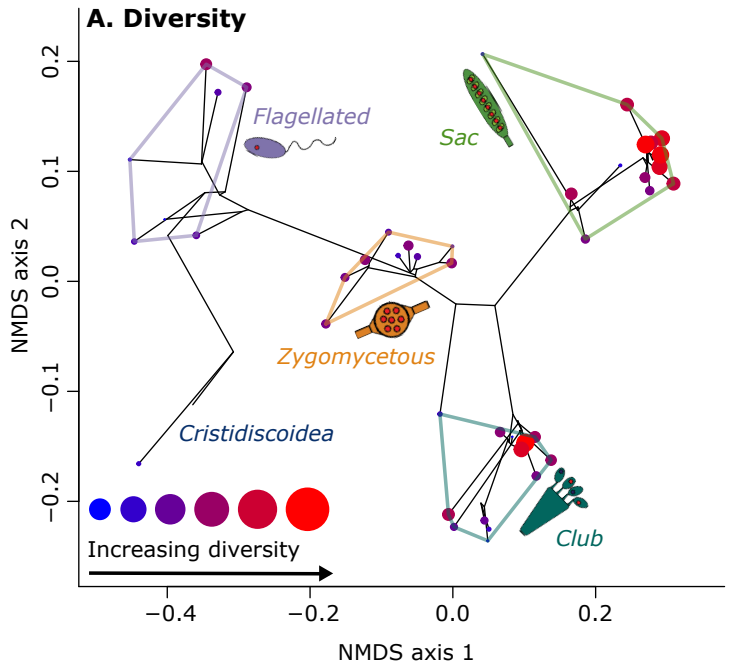
A. Diversity
Flagellated
Sac
Zygomycetous
Cristidiscoidea
Club
Increasing diversity
NMDS axis 2
NMDS axis 1

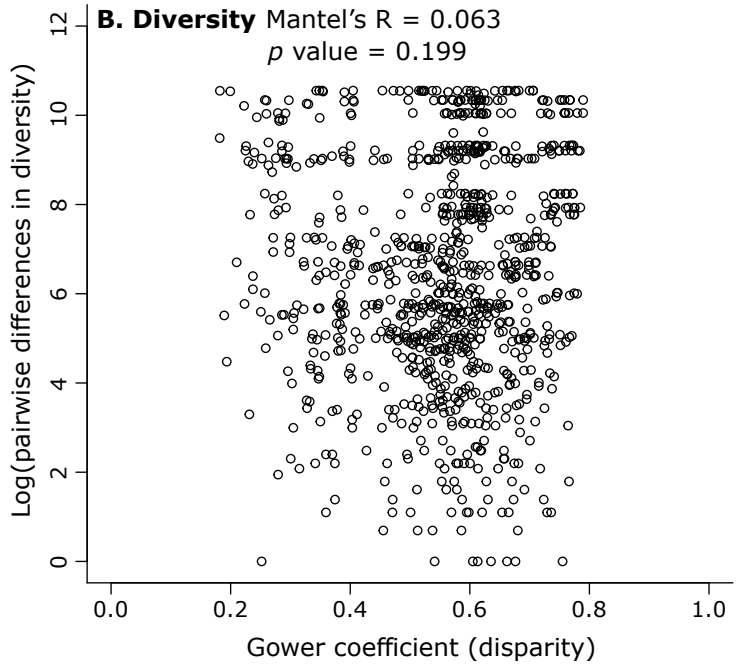
B. Diversity Mantel's R = 0.063
p value = 0.199
Log(pairwise differences in diversity)
Gower coefficient (disparity)

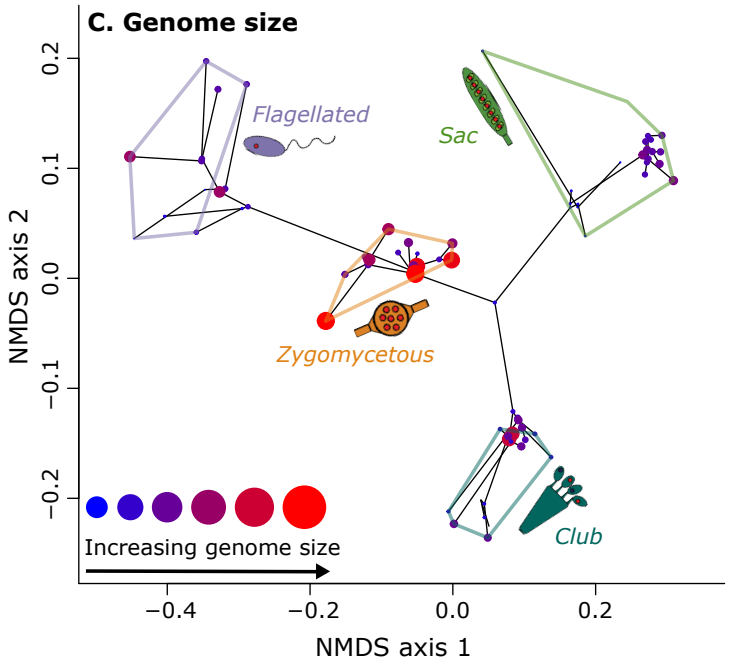
C. Genome size
Flagellated
Sac
Zygomycetous
Club
Increasing genome size
NMDS axis 2
NMDS axis 1

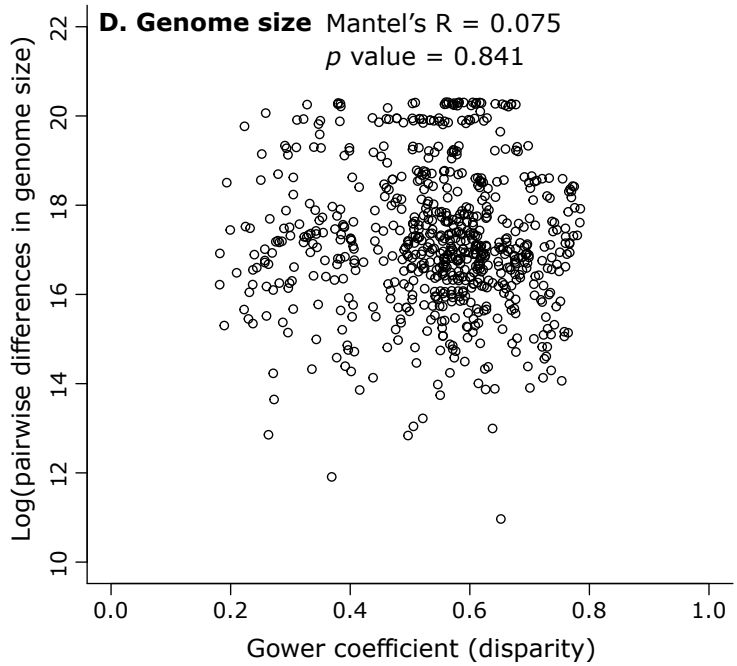
D. Genome size Mantel's R = 0.075
p value = 0.841
Log(pairwise differences in genome size)
Gower coefficient (disparity)

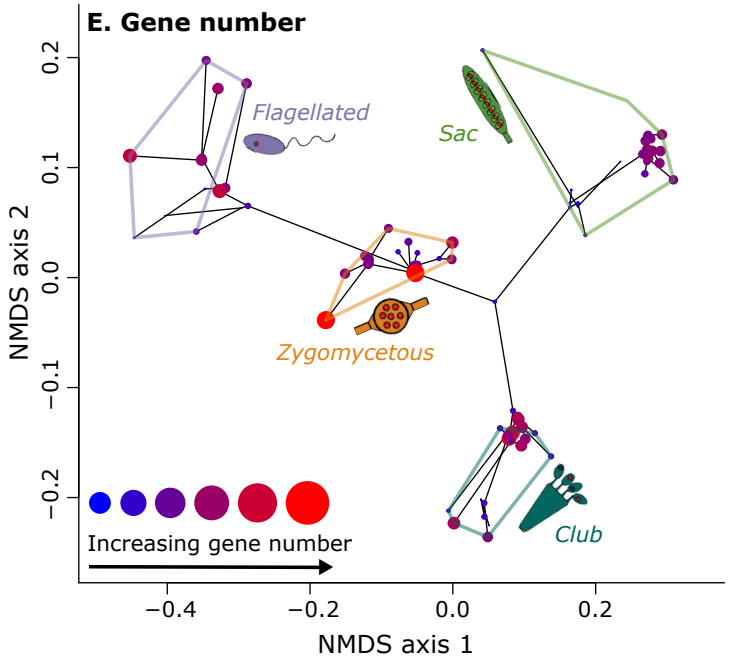
E. Gene number
Flagellated
Sac
Zygomycetous
Club
Increasing gene number
NMDS axis 2
NMDS axis 1

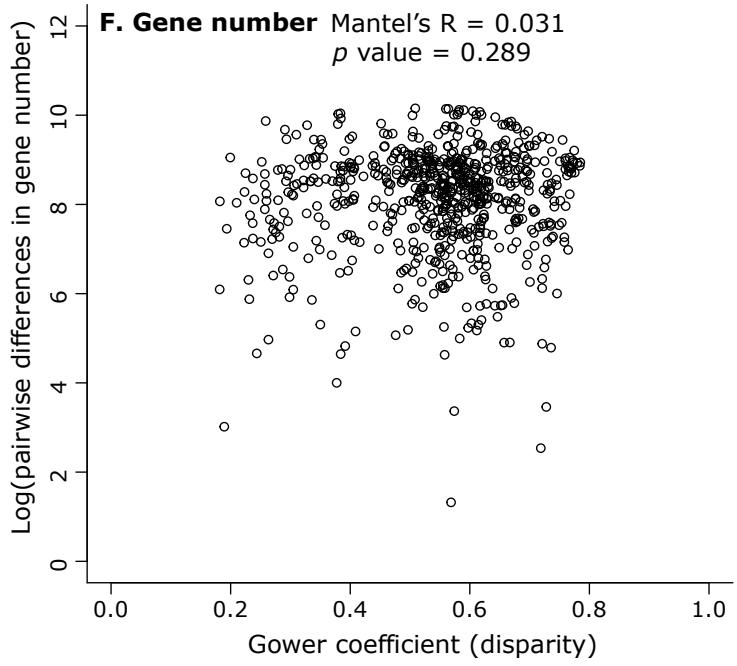
F. Gene number Mantel's R = 0.031
p value = 0.289
Log(pairwise differences in gene number)
Gower coefficient (disparity)

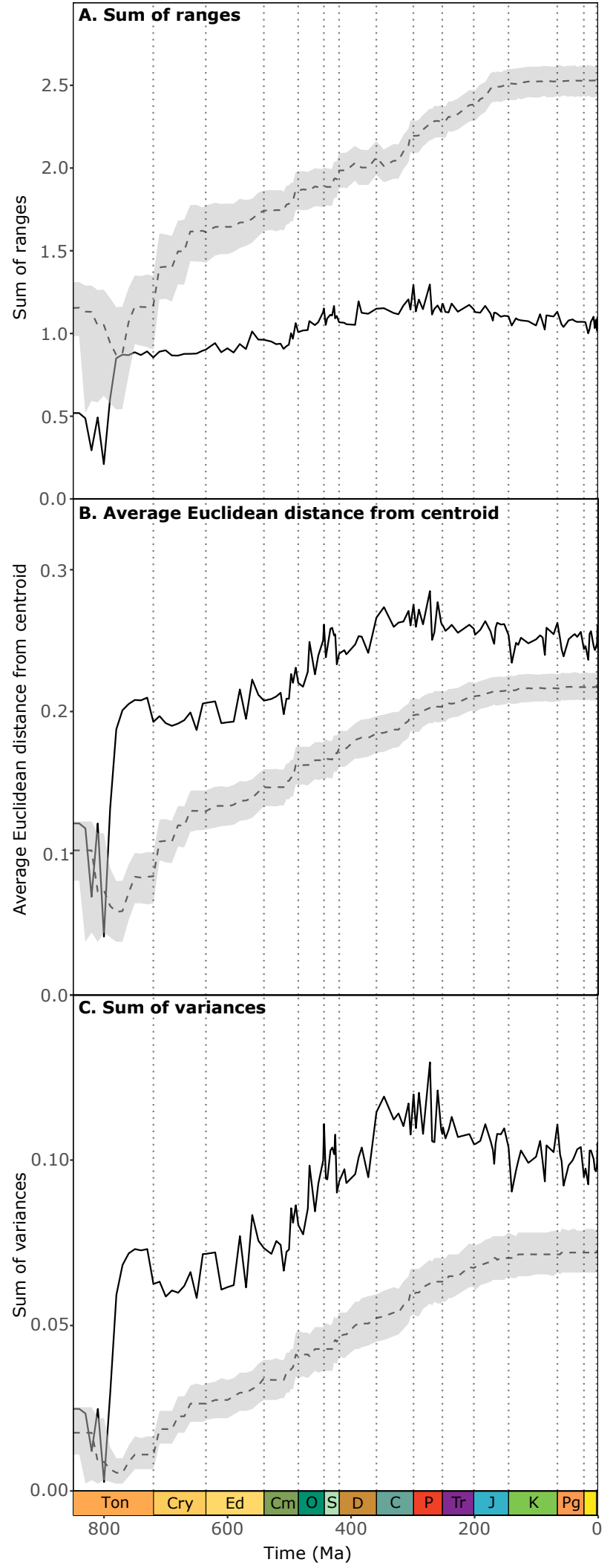
A. Sum of ranges
Sum of ranges
2.5
2.0
1.5
1.0
0.5
0.0
B. Average Euclidean distance from centroid
Average Euclidean distance from centroid
0.3
0.2
0.1
0.0
C. Sum of variances
Sum of variances
0.10
0.05
0.00
Ton
Cry
Ed
Cm
O
S
D
C
P
Tr
J
K
Pg
800
600
400
200
0
Time (Ma)

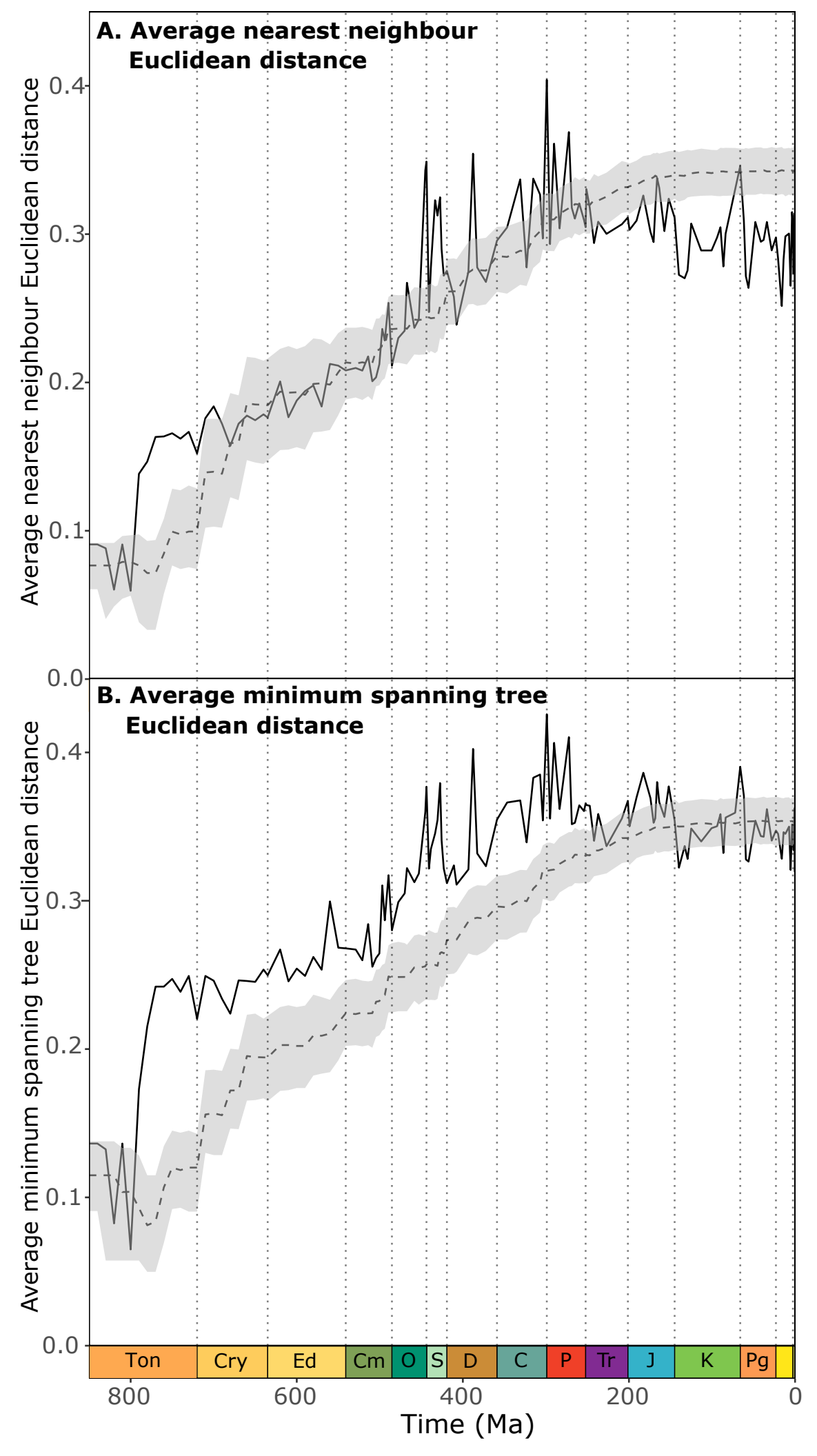
A. Average nearest neighbour Euclidean distance
Average nearest neighbour Euclidean distance
0.0
0.1
0.2
0.3
0.4
B. Average minimum spanning tree Euclidean distance
Average minimum spanning tree Euclidean distance
0.0
0.1
0.2
0.3
0.4
Ton
Cry
Ed
Cm
O
S
D
C
P
Tr
J
K
Pg
800
600
400
200
0
Time (Ma)